available at www.sciencedirect.com
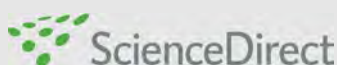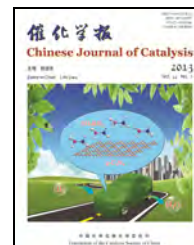
ScienceDirect

journal homepage: www.elsevier.com/locate/chnjc

Communication

Selective oxidation of toluene using surface-modified vanadium oxide nanobelts

LI Xuan[†], YE Shuang[†], ZHAO Jianbo, LI Lei, PENG Luming, DING Weiping*

Key Laboratory of Mesoscopic Chemistry of MOE, School of Chemistry and Chemical Engineering, Nanjing University, Nanjing 210093, Jiangsu, China

ARTICLE INFO

ABSTRACT

Vanadium oxide nanobelts were synthesized using a sonochemical-hydrothermal method. Hexa-decylphosphonic acid (HDPA) was introduced onto the surfaces of the nanobelts and bulk vanadium oxide to tune their catalytic properties; these properties were tested using gas-phase oxidation of toluene. The catalytic activity of the vanadium oxide nanobelts was higher than that of the bulk oxide as a result of the higher lattice oxygen activity of the nanobelts. Doping with HDPA, tuning the lattice oxygen activity, and blocking unselective sites led to both higher activity and selectivities for benzaldehyde and benzoic acid on nanobelt-like vanadium oxides, whereas led to lower activity but higher selectivities for benzaldehyde and benzoic acid on bulk vanadium oxides.

© 2013, Dalian Institute of Chemical Physics, Chinese Academy of Sciences.
Published by Elsevier B.V. All rights reserved.

Selective oxidation reactions are of great importance in transforming raw materials into intermediates and final products in the chemical industry [1]. The desired products of selective oxidation are usually sensitive to oxidation, which causes low selectivity for desired products [2]. Reactions such as the oxidation of the methyl group in toluene by molecular oxygen to give oxygenates, especially benzaldehyde, remain challenging from both the academic and industrial perspectives. The partial oxidation products of toluene, including benzyl alcohol, benzaldehyde, and benzoic acid, are commercially significant, benzaldehyde being the most valuable among them. In current industrial practice, benzaldehyde is produced via chlorination/hydrolysis of toluene or as a by-product in liquid-phase selective oxidation of toluene to benzoic acid by air [3,4]. However, these processes suffer from environmental problems because they use Cl_2 and cause equipment corrosion, and many efforts have been made in recent decades to improve catalytic

performance in the heterogeneous oxidation of toluene [3–15].

Vanadium oxide is widely used in such catalytic processes [3,8–14]. The ease of conversion among oxides with different stoichiometries and the formation of oxygen vacancies enables vanadium oxide to function as a catalyst in selective oxidation [16]. Recently, inorganic nanocrystals with well-controlled sizes and shapes have been extensively exploited, and exposed facet-function relationships have been established [17]. Moreover, molecules adsorbed as stabilizers on the nanocrystal surface have been reported to affect the catalytic activity of nanocrystals [5,18]. We have reported exclusive selectivity for benzaldehyde in toluene oxidation by molecular oxygen over oleic acid-coated CeO_2 nanocubes. This selectivity is believed to be related to surface modification by oleic acid of the well-defined CeO_2 nanocubes [5]. Centi and Perathoner [19] have discussed the possibilities of adding various organic additives to the gas phase to improve catalytic performances. Continuously dosing

the feed with pyridine during the partial oxidation of toluene on vanadium phosphate catalysts leads to significantly increased aldehyde selectivity [20]. It has also been demonstrated that self-assembled monolayers of alkylphosphonic acids on metal oxides can protect the metal from corrosion as a result of the strong chelation properties of alkylphosphonic acids [21], and nanostructured vanadium oxide exhibited unique catalytic properties in butane oxidation [22].

In this paper, we report an investigation of the surface modification of vanadium oxides by *n*-hexadecylphosphonic acid (HDPA) for the selective oxidation of toluene. Vanadium oxide nanobelts showed enhanced catalytic activity for toluene oxidation, and surface modification by HDPA increased the selectivity for partial oxidation products.

V_2O_5 nanobelts were prepared using a simple sonochemical-hydrothermal method. Bulk V_2O_5 and $NaNO_3$ were mixed in deionized water in a molar ratio of 1:1 and exposed to ultrasonic irradiation with a power of 400 W/cm^2. The mixture was then placed in a Teflon-lined autoclave at 453 K for 24 h. The resulting precipitates were thoroughly washed and dried at 333 K for 12 h. The solid was collected and designated as V_2O_5 nanobelts. Surface modification of the V_2O_5 nanobelts was carried out by immersing a sample in an ethanol solution of HDPA, with stirring, for 2 h. The solvent was removed then in an oven at 353 K. The sample with HDPA was designated as HDPA/V_2O_5 nanobelts (the HDPA surface density was about two molecules per nm^2 of V_2O_5 nanobelt surface). Bulk V_2O_5 and HDPA were mixed in deionized water in a molar ratio of 20:1 and exposed to ultrasonic irradiation with a power of 400 W/cm^2. The mixture was placed in a Teflon-lined autoclave at 453 K for 24 h. This sample was designated as V_2O_5@HDPA (the HDPA surface density was about 10 molecules per nm^2 of bulk V_2O_5 surface).

X-ray diffraction (XRD) patterns were obtained with a Phillips X'Pro diffractometer using Cu K_α radiation (λ = 0.15418 nm) at 40 kV and 25 mA. Fourier-transform infrared (FT-IR) spectra of the samples were obtained with a Bruker Vertex 70 spectrometer using KBr pellets; 64 scans were recorded, with a resolution of 4 cm^{-1}. The specific surface area was determined from N_2 adsorption at 77 K, using the BET method, on a Micromeritics ASAP-3020 instrument. H_2 temperature-programmed reduction (H_2-TPR) was performed using a TP-5080 adsorption instrument. A mixture of Ar and 4%H_2 was used and the flow rate was maintained at 20 ml/min. The H_2 consumption was monitored using a thermal conductivity detector (TCD), and the calibration of the TCD was performed by reducing a known amount of CuO to Cu^0. Temperature-programmed desorption of NH_3 (NH_3-TPD) was carried out by monitoring the NH_3 desorbed from the sample in a He flow of 31.8 ml/min, using a TCD. The samples were pretreated with He at 573 K and NH_3 was pre-adsorbed at 473 K. Transmission electron microscopy (TEM) measurements were conducted using a JEOL JEM-200CX instrument at an accelerating voltage of 200 kV. Field-emission scanning electron microscopy (FE-SEM) was performed using a Hitachi FE-SEM S4800.

In the toluene oxidation reaction, 200 mg of catalyst were introduced into a tubular quartz fixed-bed microreactor. The reaction gases were O_2 and N_2 at flow rates of 20 ml/min. Toluene was fed into the O_2 and N_2 gases using a TJ-1A syringe pump controller; the toluene:O_2:N_2 molar ratio was kept as 0.8:20:80. The gaseous products were analyzed online using a GC-9800 gas chromatograph equipped with a packed column. The organic products were collected at 273 K in anhydrous ethanol, and then analyzed using a Shimadzu GC-2014 gas chromatograph. When changing from a given experimental condition to another, a period of 1 h was allowed for reaching a new steady-state. At each temperature point, the reaction results were recorded for 4 h. CO, CO_2, benzaldehyde, benzoic acid, maleic anhydride, and phthalic anhydride were the main reaction products. The gas-phase products and organic products were quantitatively measured using relative correction factors and using *p*-xylene as an internal standard, respectively. The conversion was defined as the ratio of the number of moles of toluene converted to the number of moles of toluene fed into the reactor. The product selectivity was calculated on the basis of converted toluene.

Figure 1(a) shows typical SEM and TEM images of V_2O_5 nanobelts synthesized using a simple sonochemical-hydrothermal method. The products have belt-like nanostructures with typical lengths of up to several micrometers. The widths and thicknesses of the nanobelts are in the ranges 50–100 and 20–50 nm, respectively. Figure 1(b) shows that surface modification with HDPA does not change the morphology of the V_2O_5 nanobelts.

Figure 1(c) and 1(d) show typical electron microscopy images of the samples after the toluene oxidation reaction. The V_2O_5 nanobelts appear to be sintered to some extent during the reaction, but the morphologies of the HDPA/V_2O_5 nanobelts are basically one-dimensional structures after the toluene reaction. This implies protection by the deposition and adsorption of HDPA of the V_2O_5 nanobelts from sintering, possibly because adsorption of HDPA passivates the over-active sites on the V_2O_5 nanobelts, for example the peaks and edges. Because of the adsorption of HDPA molecules on the oxide surfaces, the specific areas of the HDPA-surface-modified catalysts cannot be
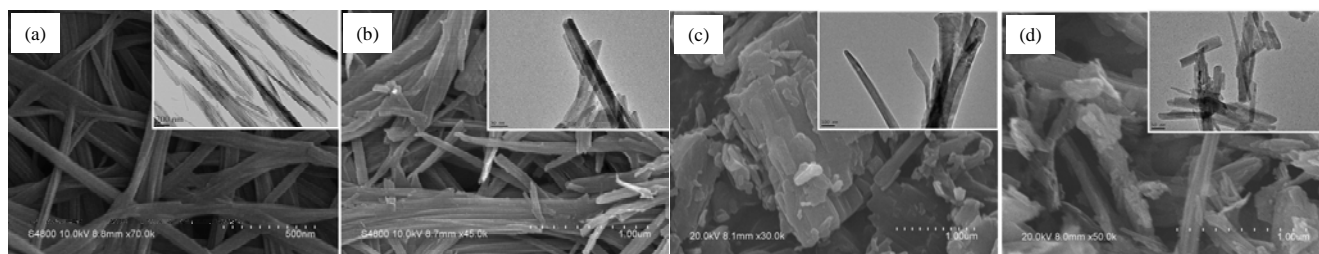

Fig. 1. SEM and TEM (inset) images of V_2O_5 nanobelts (a, c) and HDPA/V_2O_5 nanobelts (b, d) before (a, b) and after (c, d) reaction.
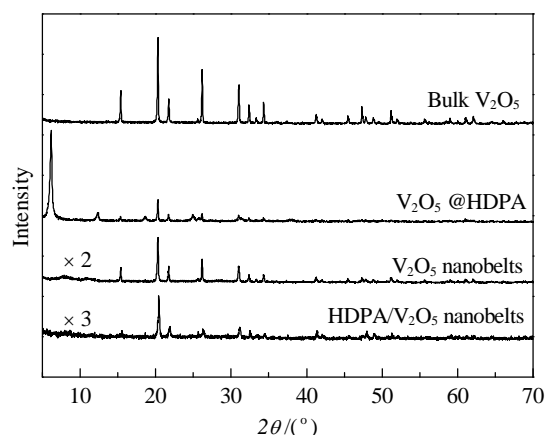
Fig. 2. XRD patterns of different catalysts.

Fig. 3. FT-IR spectra of different samples before (a) and after (b) reaction.

accurately determined; however, it is speculated that the specific areas of the HDPA-modified samples are about the same as that of the corresponding pure vanadium oxide, based on the electron microscopy images.

Figure 2 shows the XRD patterns of the catalysts; all the peaks are indexed to the V_2O_5 phase. The peaks at 6.2° and 12.3° in the V_2O_5@HDPA sample may be caused by intercalation of HDPA molecules into the lamellar structure of V_2O_5, similar to the intercalation of $VOPO_4 \cdot 2H_2O$ with 1-butanol [23]. However, there are more HDPA molecules on the V_2O_5 surface, as shown by the FT-IR spectra.

Figure 3(a) presents the FT-IR spectra of the catalysts from 3100 to 2700 cm^{-1}. The peaks at 2918 and 2850 cm^{-1} for the HDPA-modified V_2O_5 originate from methylene asymmetric and symmetric stretching modes, respectively [21]. This result indicates adsorption of HDPA on the V_2O_5 surface. Figure 3(b) shows IR peaks at 2929 and 2856 cm^{-1} from the used HDPA/V_2O_5 nanobelts and peaks at 2920 and 2850 cm^{-1} from the used V_2O_5@HDPA, indicating that the HDPA adsorbed on the catalyst surfaces is stable to some extent during the reaction. Thermogravimetric analysis (results not shown here) shows that approximately 60% of the HDPA molecules are de-
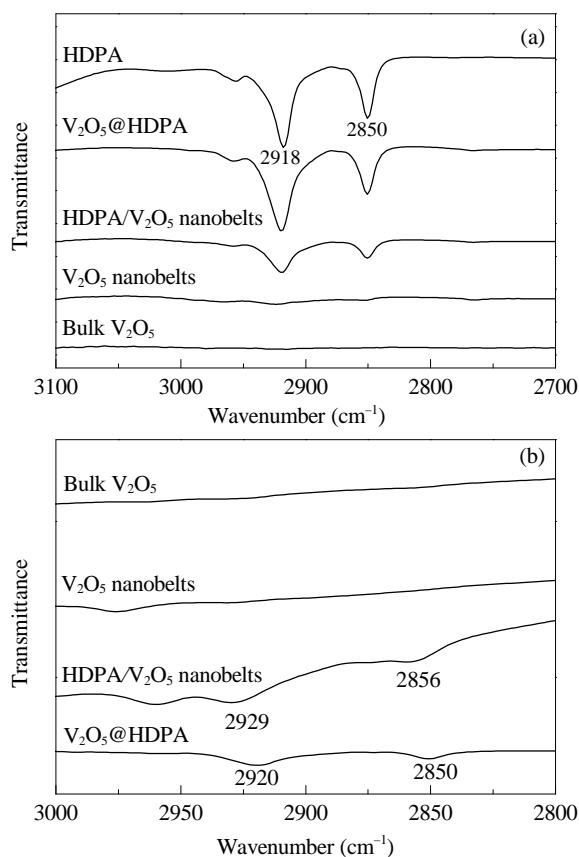
sorbed or decomposed after treatment up to 800 K in N_2. Because these catalysts are used at about 200 K below this temperature, it is assumed that a smaller amount of HDPA molecules will be desorbed or decomposed during the reaction.

Figure 4(a) shows the H_2-TPR profiles of the catalysts. The two peaks at 927 and 951 K for bulk V_2O_5 can be ascribed to the reduction of V_2O_5 to V_6O_{13} and reduction of V_6O_{13} to VO_2, respectively [24]. Interestingly, a peak at 760 K emerged for the
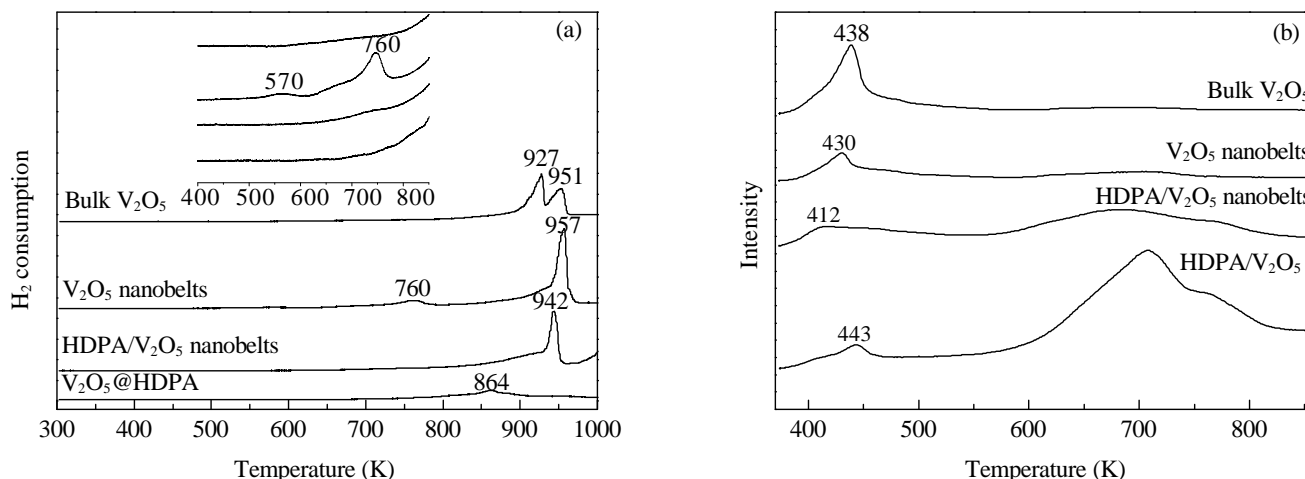

Fig. 4. H_2-TPR (a) and NH_3-TPD (b) profiles of different catalysts. The inset is a magnified profile between 400 and 850 K.

V_2O_5 nanobelt sample. Quantitative calculations for this peak show that approximately 1.5% of the oxygen atoms in the V_2O_5 nanobelts were consumed in this step. From the inset in Fig. 4(a), it can be seen that the lattice oxygen starts to be active at 400 K and forms a small peak at 570 K. We tentatively ascribe these more-active oxygen species to those located at the acme and edge areas of the nanobelts, which are commonly believed to be more active in reactions. Surface modification of the V_2O_5 nanobelts with HDPA led to the disappearance of the peaks at 760 and 570 K. This might arise from strong chelation of $PO(OH)_2$ groups with active unsaturated vanadium sites on the acmes and edges of the nanobelts. This result indicates that HDPA adsorbed on the surface of V_2O_5 nanobelts can stabilize the extremely active lattice oxygens. The lattice oxygen reactivity of V_2O_5@HDPA is significantly lower than that of bulk V_2O_5. The activity of the oxides can be controlled by adjusting the amount of HDPA adsorbed.

Figure 4(b) shows the NH_3-TPD profiles of the catalysts. In NH_3-TPD measurements, the temperature of the maximum NH_3 desorption normally reflects the relative strengths of the acid sites, and the area of the NH_3 desorption peak reflects the number of acid sites [25]. The bulk V_2O_5 exhibited a peak centered at 438 K; the V_2O_5 nanobelts had same acidity but a much smaller number of acid sites. Modification of the V_2O_5 nanobelt surfaces with HDPA caused NH_3 desorption at lower temperatures with reduced peak areas, which means both weaker acidity and fewer acid sites. The broad band from 556 to 827 K is probably the result of desorption or decomposition of HDPA on the oxide surface; this can also be seen for the V_2O_5@HDPA sample. The larger area of this broad band in the latter sample might be the result of a higher HDPA surface modification density. The HDPA/V_2O_5 nanobelts had a higher acid site density than pure oxide nanobelts did, possibly as a result of over-doping by $PO(OH)_2$ groups in HDPA onto the V_2O_5 nanobelt surfaces. Toluene and benzaldehyde have been reported to be strongly adsorbed on acid sites, leading to complete oxida-

tion to CO_x [8,20]. The effects on toluene oxidation of the surface acidities of the catalysts synthesized in this study will be discussed below.

Table 1 lists the effects of temperature on toluene oxidation over different catalysts. The conversion of toluene and selectivity for benzoic acid (BAc) increase with increasing temperature, whereas the selectivity for benzaldehyde (BA) decreases, in accordance with previous results [12,13]. V_2O_5@HDPA gives better selectivity for benzaldehyde but the lowest conversion of toluene at all tested temperatures.

At 573 K, the conversion of toluene is low (6.3%), with 67.7% and 5.1% selectivities for benzaldehyde and benzoic acid, respectively, over bulk V_2O_5. V_2O_5 nanobelts show slightly higher activity than the bulk oxide does, with a toluene conversion of 10.3%. However, the selectivity for benzaldehyde drops to 46.6%, and the selectivity for benzoic acid increases to 17.9%. It has been proven that the Mars-van Krevelen mechanism applies to gas-phase oxidation of toluene by vanadium oxide, so the main active oxygen species should be lattice oxygen [9,13,14,26]. The above-mentioned differences between the catalytic performance of bulk V_2O_5 and V_2O_5 nanobelts can therefore be explained by the higher lattice oxygen activity of the latter, which was shown by H_2-TPR (Fig. 4(a)). Surface modification of V_2O_5 nanobelts with HDPA (HDPA/V_2O_5 nanobelts) greatly increases the toluene conversion from 10.3% to 25.2% at 573 K. More importantly, the selectivity for CO_x remains at 22.9%. The lower tendency to produce total oxidation products on the HDPA/V_2O_5 nanobelts might be associated with the disappearance of the low-temperature peak in the H_2-TPR results. As discussed above, these low-temperature peaks may correspond to highly reactive lattice oxygens, which might over-oxidize toluene to CO_x. Eliminating these highly active lattice oxygen species by HDPA surface modification therefore greatly suppresses total oxidation. Moreover, V_2O_5@HDPA exhibits a much lower activity but higher selectivity for benzaldehyde, and has the highest selectivity for C_7 compounds. Also, surface modification of V_2O_5 nanobelts by HDPA gives higher selectivity for C_7 compounds when the toluene conversion exceeds 20%.

From Fig. 5, it can be seen that a low HDPA surface modification density on a nanobelt-like oxide leads to higher activity, whereas a higher modification density on the bulk oxide gives

Table 1
Catalytic properties of catalysts at different temperatures in toluene oxidation.

Catalyst	A_{BET} (m^2/g)	T/K	Conversion (%)	Selectivity (%)			
				BA+BAc	BA	BAc	CO_x
Bulk V_2O_5	16	573	6.3	72.8	67.7	5.1	14.4
		593	11.6	69.6	58.2	11.4	14.7
		613	22.7	60.7	45.7	15.1	23.5
		633	58.3	58.9	40.0	18.9	29.8
V_2O_5 nanobelts	20	553	8.8	75.3	60.9	14.4	8.9
		573	10.3	64.6	46.6	17.9	18.9
		593	20.1	51.9	27.5	24.4	29.2
		613	33.6	49.1	25.5	23.7	33.8
HDPA/V_2O_5 nanobelts	—	553	9.2	63.2	41.9	21.3	12.1
		573	25.2	59.8	28.2	31.6	22.9
		593	35.6	58.8	21.0	37.8	29.0
		613	89.0	5.5	2.1	3.3	89.1
V_2O_5@HDPA	—	593	2.7	81.4	81.4	0	8.7
		613	7.6	79.7	76.2	3.5	12.5
		633	14.1	73.3	65.1	7.2	16.8
		653	27.3	64.6	54.8	9.8	24.2

Reaction conditions: catalyst 0.2 g, toluene 0.8% (v), O_2 20% (v), N_2 79.2% (v), 20 ml/min
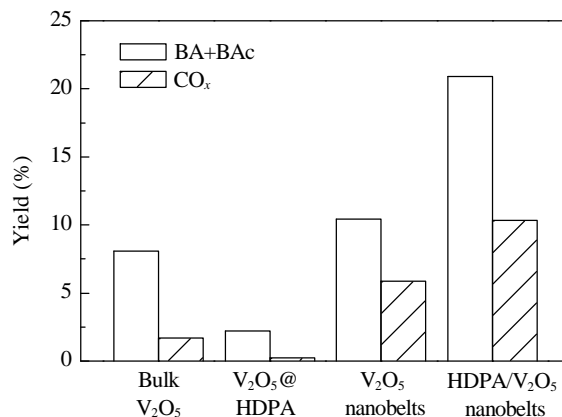BA: benzaldehyde; BAc: benzoic acid; CO_x: CO and CO_2.

Fig. 5. Catalytic performance of catalysts at 593 K.

rise to lower activity at 593 K. This indicates that the peaks centered at around 950 K in the H_2-TPR profile might be the main active oxygen species in the toluene oxidation reaction, because the V_2O_5@HDPA sample has the smallest area for this peak. The enhancing effect of HDPA modification of the nanobelts might therefore stem from tuning of the lattice oxygen activity as well as of the surface acidity. The slightly lower temperature peak at 942 K (15 K lower than for pure V_2O_5 nanobelts) in the TPR profile of HDPA-modified nanobelts may account for the increased activity, and the disappearance of the 760 K peak as well as of the active lattice oxygen species below this temperature may be the reason for the increased selectivities for benzaldehyde and benzoic acid, because these highly active oxygen species might be too reactive to control the reaction selectivity. Also, the lower NH_3 desorption temperature of 412 K (18 K lower than that for pure V_2O_5 nanobelts) might suggest easier desorption of reaction intermediates because strong acid sites adsorb benzaldehyde more strongly [8,20].

V_2O_5 nanobelts were synthesized using a two-step sonochemical-hydrothermal method. Nanostructured vanadium oxide has more-active oxygen species than the bulk oxide, leading to more total oxidation products. The surface adsorption of HDPA on V_2O_5 nanobelts significantly modifies their surface acidity and lattice oxygen activity at low temperatures. Their activity for total oxidation of toluene is suppressed and the selectivities for useful products are enhanced. The modification effects of surface adsorbents on the catalytic properties of nanostructured materials are useful for designing new catalysts and processes.

References

[1] Sheldon R A, Kochi J K. Metal-Catalyzed Oxidations of Organic Compounds. New York: Academic Press, 1981. 26
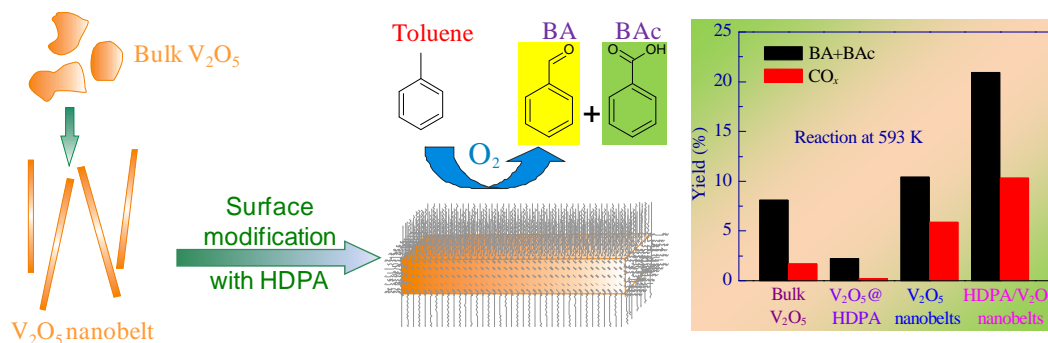[2] Hermans I, Spier E S, Neuenschwander U, Turrà N, Baiker A. *Top Catal*, 2009, 52: 1162
[3] Xue M W, Yu J N, Chen H, Shen J Y. *Catal Lett*, 2009, 128: 373
[4] Zhang Z, Gao J, Ma H, Xu J. *Chin J Catal* (张展, 高进, 马红, 徐杰. 催化学报), 2012, 33: 1198
[5] Lü J G., Shen Y, Peng L M, Guo X F, Ding W P. *Chem Commun*, 2010, 46: 5909
[6] Kesavan L, Tiruvalam R, Ab Rahim M H, bin Saiman M I, Enache D I, Jenkins R L, Dimitratos N, Lopez-Sanchez J A, Taylor S H, Knight D W, Kiely C J, Hutchings G J. *Science*, 2011, 331: 195
[7] Konietzni F, Kolb U, Dingerdissen U, Maier W F. *J Catal*, 1998, 176: 527
[8] Bulushev D A, Kiwi-Minsker L, Zaikovskii V I, Lapina O B, Ivanov A A, Reshetnikov S I, Renken A. *Appl Catal A*, 2000, 202: 243
[9] Konietzni F, Zanthoff H W, Maier W F. *J Catal*, 1999, 188: 154
[10] Bulushev D A, Kiwi-Minsker L, Renken A. *Catal Today*, 2000, 57: 231
[11] Zhang H L, Zhong W, Duan X, Fu X C. *J Catal*, 1991, 129: 426
[12] Xue M W, Ge J Z, Zhang H L, Shen J Y. *Appl Catal A*, 2007, 330: 117
[13] Ponzi M, Duschatzky C, Carrascull A, Ponzi E. *Appl Catal A*, 1998, 169: 373
[14] Ge H, Chen G W, Yuan Q, Li H Q. *Chem Eng J*, 2007, 127: 39
[15] Kuang W X, Fan Y N, Chen K D, Chen Y. *J Catal*, 1999, 186: 310
[16] Haber J. *Catal Today*, 2009, 142: 100
[17] Zhou K B, Li Y D. *Angew Chem, Int Ed*, 2012, 51: 602
[18] Narayanan R, El-Sayed M A. *J Phys Chem B*, 2005, 109: 12663
[19] Centi G, Perathoner S. *Catal Today*, 1998, 41: 457
[20] Martin A, Bentrup U, Lücke B, Brückner A. *Chem Commun*, 1999: 1169
[21] Gao W, Dickinson L, Grozinger C, Morin F G, Reven L. *Langmuir*, 1996, 12: 6429
[22] Taufiq-Yap Y H, Wong Y C, Zainal Z, Hussein M Z. *J Nat Gas Chem*, 2009, 18: 312
[23] Yamamoto N, Hiyoshi N, Okuhara T. *Chem Mater*, 2002, 14: 3882
[24] Besselmann S, Freitag C, Hinrichsen O, Muhler M. *Phys Chem Chem Phys*, 2001, 3: 4633
[25] Due-Hansen J, Kustov A L, Rasmussen S B, Fehrmann R, Christensen C H. *Appl Catal B*, 2006, 66: 161
[26] Mars P, van Krevelen D W. *Chem Eng Sci*, 1954, 3(supple 1): 41

Graphical Abstract

Chin. J. Catal., 2013, 34: 1297–1302   doi: 10.1016/S1872-2067(12)60619-6

Selective oxidation of toluene by surface-modified vanadium oxide nanobelts

LI Xuan, YE Shuang, ZHAO Jianbo, LI Lei, PENG Luming, DING Weiping*
Nanjing University

Vanadium oxide nanobelts are more active, but less selective, in toluene oxidation than bulk vanadium oxide is. Significant modification of the selective oxidation of toluene on vanadium oxide nanobelts is achieved by doping with hexadecylphosphonic acid.

表面修饰的钒氧化物纳米带上甲苯选择氧化反应

李　轩[†], 叶　霜[†], 赵建波, 李　磊, 彭路明, 丁维平[*]

南京大学化学化工学院, 介观化学教育部重点实验室, 江苏南京210093

摘要: 采用声化学水热法制备了V_2O_5纳米带, 并将十六烷基膦酸负载在它和块状V_2O_5表面上, 以修饰催化剂表面, 通过调变催化剂中晶格氧活动性以及表面酸碱性来控制其催化甲苯氧化产物的选择性. 结果表明, V_2O_5纳米带具有较强的晶格氧活动性, 与普通块状V_2O_5相比, 甲苯转化率更高, 但苯甲醛和苯甲酸的总选择性下降. 经过表面修饰后, V_2O_5纳米带的催化活性以及苯甲醛、苯甲酸总选择性增加; 而块状V_2O_5上苯甲醛、苯甲酸总选择性更高, 但催化活性显著下降.

关键词: 五氧化二钒纳米带; 选择氧化; 甲苯; 十六烷基膦酸; 表面修饰